OBSERVATIONS OF LANGMUIR CIRCULATION, WAVES AND THE MIXED LAYER

Jerome A. Smith
Scripps Inst. Oceanography, La Jolla, CA 92093-0213 USA

Abstract. Doppler sonar observations of surface velocity are analysed to extract an rms velocity scale related to flow patterns persisting for at least a minute, and having advection velocities within an adjustable "window" of the mean advection rate. The resulting velocity scale is related to the wind and waves over the course of the twenty days available from the SWAPP data set. The correlation with the wind is good, but the inclusion of a predicted wave dependence increases the correlation.

1 Introduction.

Langmuir circulation is an easily recognizable form of "coherent structure," often seen on the surface of large bodies of water. This form, as first described by Langmuir (1938), consists of a series of "roll vortices" within the mixing layer, of alternating sign and with axes roughly parallel to the wind. It is easily recognized because this form of circulation tends to draw materials floating at the surface into "windrows," long linear surface features roughly aligned with the wind (Figure 1). Although it is hard to substantiate quantitatively, this form of circulation appears to occur more often in the surface boundary layer of oceans and lakes than in the analogous layer of the atmosphere. It is currently suspected that effects due to the presence of surface waves may account for this difference.

In February and March of 1990, a deep sea experiment took place called the "Surface Wave Processes Program" (SWAPP; figure 2). One goal of this study is to characterize Langmuir circulation in the mixed layer of the open ocean over a variety of conditions, and to relate the observed characteristics to the circumstances in which they arise: 1) Existence (when do they occur?); 2) Strength (e.g., an RMS velocity scale associated with the motion); 3) The spacing between convergence zones ("windrows"), or the heirarchy of scales if such exists; 4) The orientation of the rolls with respect to both the wind and the waves (and possibly also with respect to planetary rotation, or North); and 5) The relevent depth scales, or the "shape" in vertical cross-section. Of these long-term objectives, this paper is concerned mainly with number 2, the strength, and the relation of this to forcing by both wind and waves.

2. The data and circumstances

The discussion here centers on data taken with a Doppler sonar system, oriented to measure a velocity component along the surface along each of 4 lines, spaced azimuthally in 45° increments (figure 3). The system measures velocity in 3 m "range bins" extending some 350 m along each of these lines. It was used to measure both surface wave directional spectra and the lower frequency motions

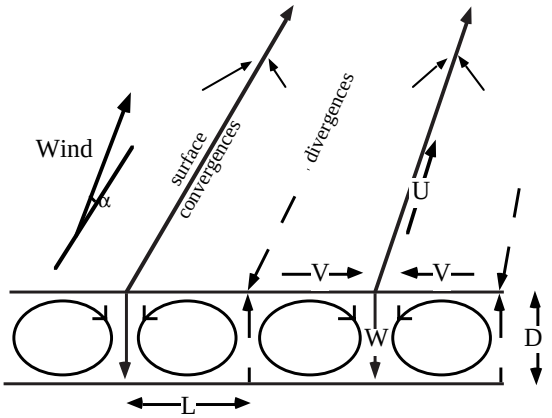

Fig. 1. A schematic view of Langmuir circulation. The convergence "stripes" are observed to lie within 20° or so of the wind direction. The velocity scales are a percent to a few percent of the windspeed.

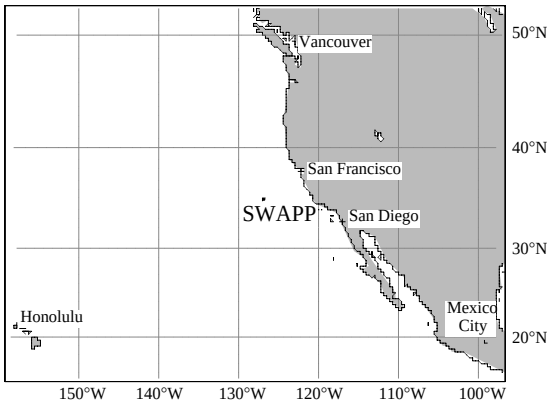

Figure 2. The location of SWAPP, in deep water some 500 km off the coast of California.

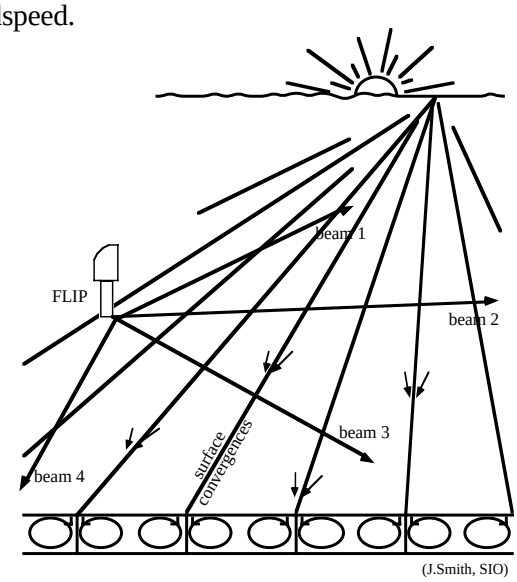

Fig. 3. Schematic view of Langmuir circulation and the 4 sonar beams extending from FLIP.

such as those associated with Langmuir circulation. A description of the system and operating parameters is given in Smith (1992); the design and perfomance characteristics are discussed in Smith (1989) and Pinkel and Smith (1992). For the main purpose here of describing the strength of Langmuir circulation over the duration of the experiment, it was found that one-minute averages of velocity are adequate. Two samples of one-minute averaged sonar data are shown in figure 4. The two are from the wind event just before "day 65" (yearday, 1990), and provide examples of developing and fully developed Langmuir circulation, respectively. For the supplementary surface wave information, directional spectra of the surface wave field were estimated at least every two hours from an hour's worth of data.

Another important ancillary piece of information is the wind. Windspeed and direction, and the corresponding bulk-formula windstress (including corrections based on estimated heat flux and stability), were provided by R. Weller and A.

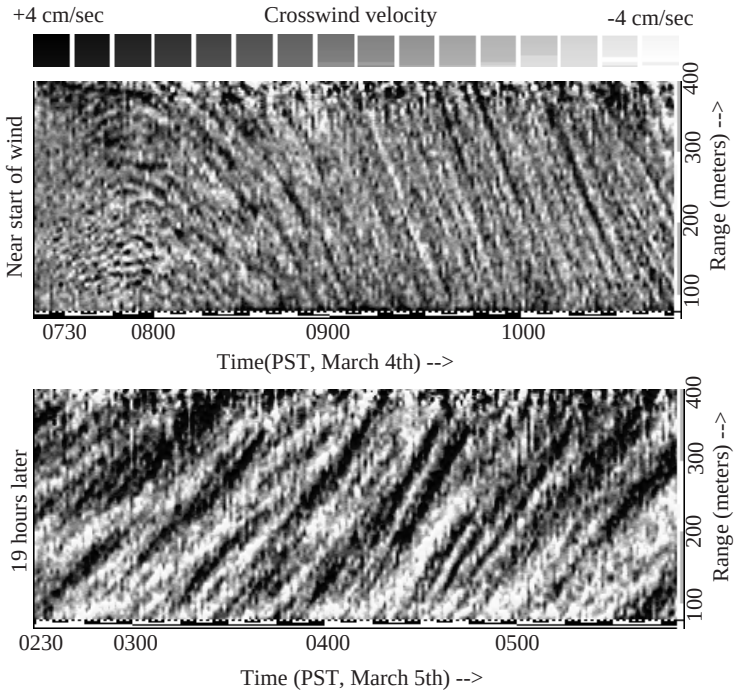

Figure 4. Two samples of sonar velocity data from SWAPP. The first sample is near the beginning of a wind event. The wind increased suddenly at about 7:30; just after that, small "ripples" are apparent, especially near 150m range. After that, there is rapid evolution toward larger scales; also the mean flow increases, creating the diagonal stripes seen over the second half of this sample. The second sample is some 19 hours later, and shows "fully developed" Langmuir circulation.

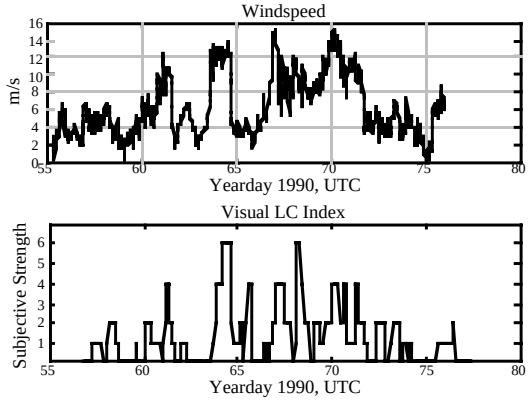

Figure 5. a) The windstress magnitude (provided by Weller and Plueddemann, WHOI). b) A "visual index" of Langmuir circulation, based on examination of both intensity and velocity data from the sonars (estimated by R. Weller, WHOI).

Plueddemann of Woods Hole Oceanographic Institution (figure 5a).

Both the sonar and the weather measurements were made from the R/P FLIP, which was moored at 35° N, 127° W, about 500km off the coast of California, at a 4000m deep part of the Pacific ocean (figure 2). Over the course of the experiment, the wind rose above 10 m/s on four occasions, reaching 15 m/s twice. A "visual index" of Langmuir circulation existence and strength was devised, based on a combination of data including the tendency and speed with which computer cards lined up on the ocean surface, and on range-time maps of sonar intensity and velocity (figure 5b). The index ranges from 0 (no circulation observed) to 6 (for very well pronounced streaks, in visual observations of both

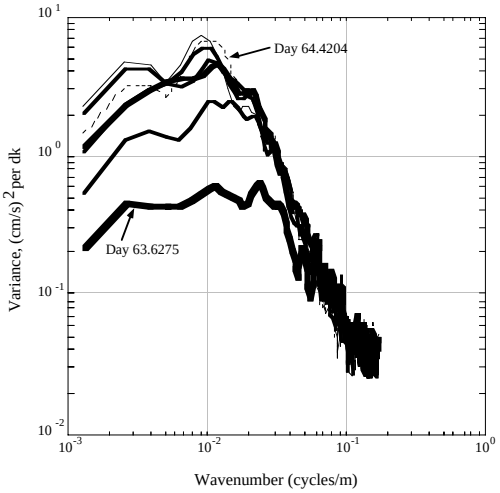

Fig. 6. Time-lagged cospectra of velocity from the Doppler sonar data. Six hour averages, 3 hour intervals displayed.

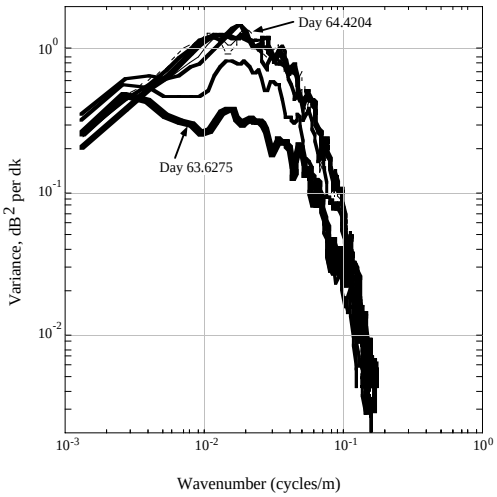

Fig. 7. Time-lagged cospectra of acoustic backscatter intensity, as in figure 6 for velocity. Note the difference in spectral form.

the sea surface itself and the sonar data). We shall return to this visual index later as a form of "ground truth" for the objectively analysed index, to be discussed.

3. Double-lagged cospectra

We wish to distinguish velocity variance associated with persistent features in the surface layer from that due to other forms of "turbulence" and surface waves. The former will be assumed to reflect mainly Langmuir circulations, and so can be used as an objective measure of the strength of circulation, for comparison to windstress and surface wave conditions.

To this end, cospectra are formed for each beam from spatial FFTs of each one-minute averaged transect. First, the inner products of the coefficients at each time with those for one minute later are formed:

$$A(k,t) \equiv \int v(r,t)\, e^{-ikr}\, dr \;\equiv R\, e^{i\phi} \tag{1}$$

$$C(k,\Delta t) \equiv \langle\, A^*(k,t)\; A(k,t+\Delta t)\,\rangle \tag{2}$$

The resulting products are further averaged over one hour time-periods. These are referred to as "one minute time-lagged cospectra." Examples of a such time-lagged cospectra are shown in figure 6, from the time period at the beginning of the wind event before day 65 (sometimes referred to as "the March 4th event"). These example spectra show an increase in time at low wavenumbers, as the Langmuir circulation becomes more "fully developed" after the start of the wind. Also, note that the spectral slope at high wavenumbers appears to fall roughly as k^{-2} over an "equilibrium range" extending to the noise floor of the sonar data.

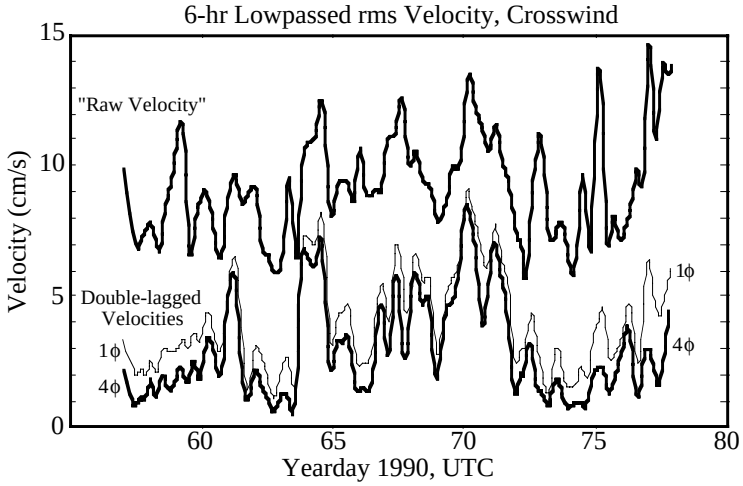

Fig. 8. The noise reduction effected by the "Double-lagged covariance" processing (see text).

A similar analysis may be performed on acoustic backscatter intensity data. The time-lagged cospectra of intensity are shown in figure 7 for the same times as in figure 6. The shape of the intensity spectrum is rather different from that of velocity. In particular, the largest (dominant) scale in the velocity figure approaches 0.009 cycles per meter (cpm), but there is no corresponding peak in the intensity spectra; instead the intensity spectra peak at higher wavenumbers (if at all), near 0.02 cpm. Since velocity is probably more dynamically relevent, the intensity data will not be discussed further.

For such time-lagged cospectra, the phases "$\Delta\phi$" of the cospectral coefficients are directly related to the frequencies of the associated motion: $\omega(k) = (\Delta\phi/\Delta t)$ (as long as the change in phase over Δt is "comfortably less than" π). For features which are approximately "frozen" into the mixed layer, the frequency so measured would increase in direct proportion to the wavenumber "k". Thus, it is advantageous to take the derivative (effectively) of the phase with respect to k:

$$D(k+\Delta k/2,\Delta t) \equiv C^*(k,\Delta t)\ C(k+\Delta k,\Delta t) \qquad (3)$$

so $|D| \propto R^4 \propto (v^2 \text{ per } dk)^2$, and $\text{angle}(D) \propto \Delta\phi/(\Delta k\ \Delta t)$. In other words, the phase of this new "double-lagged" coefficient "D" is proportional to a "group velocity" along the beam, which would be constant for a "frozen field" of features advected past at a constant speed. As a result, the coefficients can be summed coherently over all scales, yielding measures of both the "total coherent velocity variance" and the advection rate along the beam.

Before summing, there are two further possible adjustments, facilitated by separating the "D" coefficients into magnitude and phase. First, to restore the units to velocity variance density (v^2 per dk), the square-root of the magnitude is taken. Second, the phase of "D" can be multiplied by a positive integer. This has the effect of tightening the deviation from the mean velocity which is "tolerated" in the coherent sum. For example, in the present data set, $\Delta t = 60$s and $\Delta k = 2\pi/R = 2\pi/768$m; thus, a phase of $\pi/2$ corresponds to a velocity of 3.2 m/s. Clearly, with advection speeds an order of magnitude smaller than that, this "velocity window" could be tightened up considerably. Multiplying

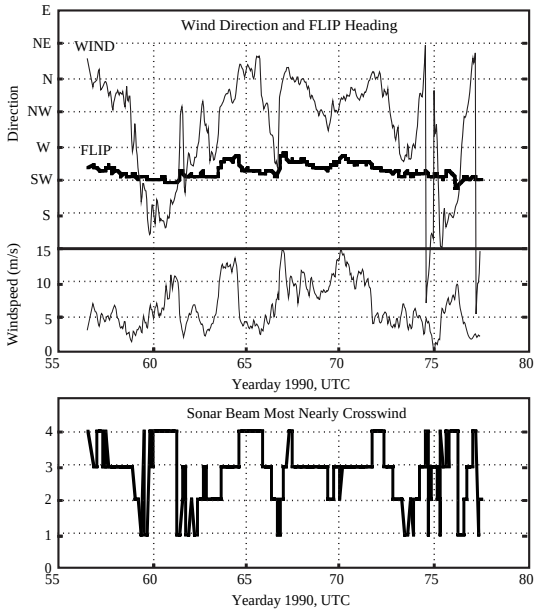

Fig. 9. Wind and FLIP headings, and the most nearly crosswind beam.

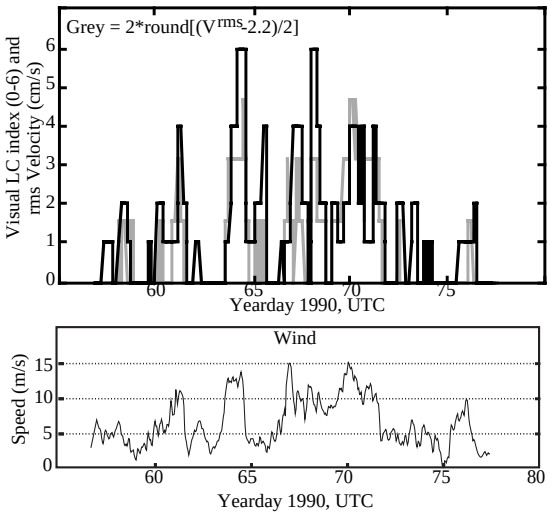

Figure 10. Comparison of the visual "LC index" with one derived from the rms velocity in the cross wind direction.

the phases of the "*D*" coefficients by 4 reduces the velocity window to 0.8 m/s, more in line with the typical advection rates. With this adjustment, variance in the cospectrum corresponding to group velocities differing from the weighted mean by more than 0.8 m/s are likely to be averaged out.

The "noise" in the estimated velocity variance is reduced two ways: first by enforcing a one-minute (or longer) persistence time, and second by enforcing conformity of the apparent advection rate to within a limit surrounding the "weighted mean advection rate." The "noise filtered" velocity variance over the course of the experiment is illustrated in figure 8, and compared to both the unfiltered velocity (terrible) and to the windstress (a reasonable correlation is evident).

4. Crosswind velocities and the LC index

The next problem to be sorted out is which of the 4 sonar beams is most nearly oriented directly across the linear features associated with Langmuir circulation (see figure 3 again). Since the windrows are observed to lie generally along the wind direction, the (one-hour averaged) wind direction is used here as a reference. Using the headings of both the wind and FLIP, the sonar beam aimed most nearly across the wind is selected (figure 9), and the velocity variance associated with that beam is retained for the "LC index" of interest here. After this selection, the one-hour averaged data is further filtered to an effective 6-hour sample rate (12 hour Nyquist frequency).

The aim is to compare this "rms velocity index" (V^{rms}) with the visual LC index referred to above. To account for a finite "noise floor" in the rms velocity estimates, a small value is first subtracted (2.2 cm/s); then the velocity

time series is rounded to the nearest even integer, to match the effects of the subjective assignment of the visual index (it is noted that, over the whole data series, an overwhelming majority of the subjectively picked values are even). It is pure coincidence that the amplitudes of the two "indices" match, with 1 cm/s in V^{rms} per "point" on the visual index (in fact, a slightly better correlation is obtained with a scale factor of about 1.05 cm/s per point; the difference is not significant, however). As shown in figure 10, the match is fairly convincing. The overall correlation between the visual index and the rounded rms velocity (with 6 hr smoothing) is 0.7175. For a short period near the beginning of the experiment, on days 56 and 57, the visual index indicates a weak presence of Langmuir circulation, while the rms velocity index remains at zero; near day 74 a similar mismatch occurs. Thus, there is a slight suggestion that the weakest circulations are "under-represented" in the rms velocity index.

It is surprising that an index based solely on V^{rms} matches the visual index so well. The latter is based not just on the strength of the velocity associated with the features, but also on the "orderliness," the scale of the "stripes" occuring in the time-range plots, and a view of the backscatter intensity data as well as velocity. Over the course of the time series, the maximum or dominant scale of the circulations varies significantly (e.g., as gauged by the peak in the wavenumber spectra, or in the spacing between the largest convergence zones). One would expect this to influence the match.

The subjectively good match between V^{rms} as a scale and the visual index is taken as evidence that, for the most part at least, V^{rms} as derived and discussed here does, in fact, relate to Langmuir circulation. It is therefore useful to press on and relate this V^{rms} to the wind and wave climate. How should one expect the cross-wind velocity to vary with wind, waves, and the scale of the circulation?

5. Scaling of the surface cross-wind velocity by wind and waves.

A theory currently thought to be most relevent to the generation of Langmuir circulation in the surface layers of oceans and lakes was derived in rather different but complementary forms by Craik and Leibovich (1976) and by Garrett (1976) (see, for example, Leibovich 1980). The former is more mathematically rigorous, and begins with a carefully ordered scaling of the various dynamics of possible importance. In this formulation, the crosswind velocity is effectively scaled by $(U^s w^{*2})^{1/3}$, where U^s is the velocity of the wave-induced Lagrangian drift at the surface (the "surface Stokes' drift"), and w^* is the "friction velocity" associated with the windstress, $\tau = \rho w^{*2}$ (here the friction velocity in the water is used). It does not depend on the length scale of the associated circulation. But how does this scaling arise? Is it logical that the scale of circulation doesn't influence the velocity scale?

We may quickly re-argue the scaling as follows. First, assume that a constant fraction of the total momentum transport through the mixed layer is accounted for by the circulation (for example, 100%). Then

$$\tau/\rho = \langle u'w' \rangle \propto UW \propto (D/L)\, UV, \text{ or } U \propto (L/D)\, w^{*2}/V, \qquad (4)$$

where U, V, and W are the alongwind, crosswind, and vertical velocity scales of the Langmuir circulation, and L and D are the crosswind and vertical length scales, respectively. Next, from the theory mentioned, we take the crosswind forcing at the surface to be given roughly by

$$M\times(\nabla\times U) \approx U^s U_y \approx U^s U/L \approx U^s w^{*2}/DV \equiv F_\perp \tag{5}$$

where M is the wave momentum (this is the "keystone" in this scaling argument). Finally, we let the crosswind velocity scale be determined by the time (scale) the water at the surface is exposed to this force before reaching the convergence and being subducted:

$$V \propto TF_\perp = (L/V)F_\perp = (U^s w^{*2}/V^2)(L/D), \text{ or} \tag{6}$$

$$V \propto (U^s w^{*2})^{1/3}(L/D)^{1/3} \approx (U^s w^{*2})^{1/3}. \tag{7}$$

It is seen that the length scales drop out of the cross wind velocity scaling (except for the vertical to crosswind aspect ratio). Since the possible behavior of this aspect ratio is unknown, the discussion will proceed with the tacit assumption that the aspect ratio doesn't vary significantly or systematically.

This scaling result provides only a weak basis for experimental verification. Without the wave forcing, the only relevent scale would be w^*; the above result differs from this by just $(U^s/w^*)^{1/3}$. In general, the surface Stokes' drift, which is influenced strongly by waves of moderately high frequency, tracks the wind closely.

The angular deviation between the wind and waves should also be taken into account. If we assume that the circulation pattern aligns roughly halfway between the wind and wave directions, this would introduce an additional factor of $[\cos^2(\Delta\theta/2)]^{1/3}$ to the velocity scale, where $\Delta\theta$ is the angle between the wind and waves. Here, since the Stokes' drift tracks the wind so well, this factor is found to have negligible influence on the results (but is included anyway).

In this experiment, the sonar system was also used to measure waves of periods longer than about 2 seconds. It is straightforward to compute directional spectra and hence, through linear wave theory, the surface Stokes' drift (figure 11). Over the whole time series, the ratio $(U^s/w^*)^{1/3}$ remains fairly constant, between 1 and 2 (figure 11c). Ignoring times when w^* and U^s are small (i.e., on days 59, 63, and 75), the most significant deviation from this roughly constant value occurs on day 65, when the wind dies suddenly while the Stokes' drift remains high.

6. Results

To evaluate this scaling, compare the results of scaling V^{rms} by just w^* versus scaling it by $(U^s w^{*2})^{1/3}$ (Figure 12). The squared correlation between V^{rms} and w^* over the whole timeseries is 0.9205; the squared correlation between V^{rms} and $(U^s w^{*2})^{1/3}$ is 0.9337 (no means removed). For geophysical properties,

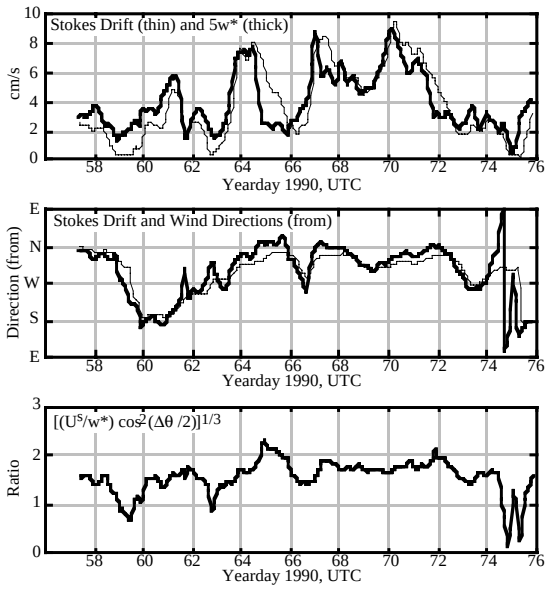

Fig. 11. Surface Stokes' drift (U^S) and water friction velocity (w*) over the course of SWAPP, smoothed with a 6 hr running mean. (a) Magnitude; (b) Direction; (c) Ratio of scaling factor to w* (see text).

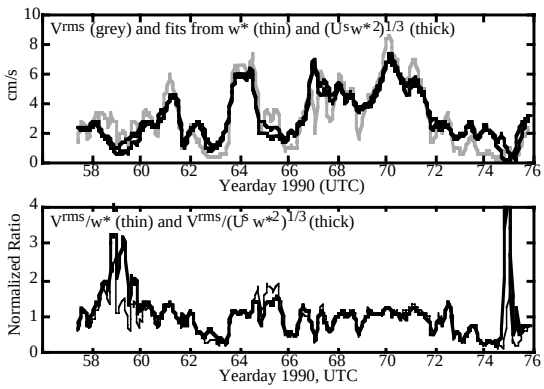

Fig. 12. Comparisons between V^{rms} (grey) and fits from just w* (thin lines) versus the theoretical scaling $(U^S w^{*2})^{1/3}$ (thick lines). (a) V^{rms} and the scaling fits; (b) The ratio of V^{rms} to the scaling fits. Ignoring times when all three are small (days 59, 63, and 75), the only significant difference occurs on day 65, when the Stokes' drift remains anomolously high.

both correlations are quite high. The residual variances are 8.33% for the *w** scaling, and 6.54% for the theoretical scaling. This reduction of the residual variance is statistically significant to well over 95%, given about 80 degrees of freedom for these estimates (20 days of 6 hr averages). From inspection of Figure 12, it is apparent that the difference in correlation values arises almost entirely from day 65, when the anomolously high Stokes' drift occurred.

Overall, it appears that: (1) scaling by *w** alone does a good job, with no time delay, of describing V^{rms}; and further (2) scaling by $(U^S w^{*2})^{1/3}$ does a better job, indicating that waves are somehow affecting the motion.

The improvement in fit by including the wave term is not large, but it is significant. This is the first piece of direct evidence that the waves are involved somehow in determining the strength of circulation in the mixed layer. While this supports the theory mentioned above, it falls far short of "proving" it. Indeed, there are many other ways one can think of by which the waves could be indirectly influencing these structures. For example, the increased wave breaking could simply increase the level of turbulence in the mixed layer, providing a "richer" cascade of energy to these larger scales. Or, the varying wave conditions could influence the windstress, changing it from the "bulk formula" value (however, in this case, one might argue that the largest deviations should occur near the beginning of each wind event, when the waves are "younger" and steeper, rather than afterwards, during a "lull"). Nevertheless, it is an encour-

aging piece of evidence. The discussion here has centered on the first two of the five long-range goals: the existence and strength of Langmuir circulation. Much remains to be done, particularly on the length scales and orientation of the rolls, both along the 2D surface plane and in a "vertical cut" across the rolls.

7 Acknowledgements

This work was supported by ONR grants N00014-90-J-1285 and N00014-93-1-0359. I wish to thank R. Weller, A. Plueddemann, A. Gnanandesikan, and S. Thorpe for useful discussions.

References

Craik, A. D. D., and S. Leibovich, A rational model for Langmuir circulations, *J. Fluid Mech.*, *73*, 401-426, 1976.

Garrett, C. J. R., Generation of Langmuir Circulations by surface waves - A feedback mechanism, *J. Mar. Res.*, *34*, 117-130, 1976.

Langmuir, I., Surface motion of water induced by wind, *Science*, *87*, 119-123, 1938.

Leibovich, S., On wave-current interaction theories of Langmuir circulations. *J. Fluid Mech.* *99*:715-724, 1980.

Pinkel, R., and J. A. Smith, 1992: Repeat sequence codes for improved performance of Doppler sounders. *J. Atmos. Oceanic Technol.*, **9**, 149-163.

Smith, J. A., 1989: Doppler sonar and surface waves: Range and resolution, *J. Atmos. and Oceanic Tech.*, **6**, 680-696.

Smith,J.A.,1992, 'Observed growth of Langmuir circulation,'*J.Geophys Res.* **97**, 5651-5664.